Exfoliation and Restacking Route to Anatase-Layered Titanate Nanohybrid with Enhanced Photocatalytic Activity

Jin-Ho Choy,*,[†,‡] Hyun-Cheol Lee,[†,‡] Hyun Jung,[†,‡] Hasuck Kim,[‡] and Hankil Boo[‡]

National Nanohybrid Materials Laboratory and School of Chemistry and Molecular Engineering, Seoul National University, Seoul 151-747, Korea

A new microporous TiO_2-pillared layered titanate has been prepared by hybridizing the exfoliated titanate with the anatase TiO_2 nanosol. The stable colloidal nano-sheet was obtained by intercalating tetrabutylamine into the layered protonic titanate, $H_xTi_{2-x/4}\square_{x/4}O_4 \cdot H_2O$ ($x = 0.67$), with a lepidocrocite-like structure. The colloidal suspension of exfoliated titanate sheets was mixed with the monodispersed anatase TiO_2 nanosol solution prepared by the hydrolysis of titanium isopropoxide with acetylacetone. The obtained nanohybrid was heated at 300 °C for 2 h in order to complete the grafting reaction of intercalated anatase TiO_2 nanosol on the interlayer surface of layered titanate. According to the X-ray diffraction analysis and N_2 adsorption−desorption isotherms, it was found that the TiO_2-pillared layered titanate showed a pillar height of ∼2 nm, a high surface area of ∼460 m²/g, and a pore size of ∼0.95 nm, indicating the formation of a microporous pillar structure. Its photocatalytic activity was evaluated by measuring the total volume of H_2 gas evolved during the irradiation of the catalyst suspensions in water. The H_2 gas evolution was found to increase from the layered titanate (cesium and protonic form) to the unsupported TiO_2 (acac-TiO_2) and the TiO_2-pillared layered titanate, because the electron and hole recombination in the pillared system is thought to be effectively suppressed because of electron transfer between guest and host. A marked enhancement in the activity by ca. 40 times was obtained for TiO_2-pillared layered titanate compared to pristine compounds such as layered titanate and anatase TiO_2 nanosol when Pt (0.3 wt %) was doped on the surface of the sample.

Introduction

Photocatalytic reactions of semiconductors, such as evolution of hydrogen gas from water or oxidative degradation of organic pollutants, have attracted intense research interest because of their possible application to the conversion of solar energy into chemical energy.[1] TiO_2 is one of the most extensively studied semiconductors for such photocatalytic reactions because of its low cost, ease of handling, and high resistance to photoinduced corrosion.[2,3] However, TiO_2 is a wide band gap semiconductor that only adsorbs photons in the near-UV region, thus limiting its use in solar-based applications. Recently, there has been considerable interest in nanohybrids which often exhibit extraordinarily high synergetic and complementary behavior between two component materials.[4,5] In particular, the combination of two-dimensional layered materials and intercalation techniques offers novel

approaches for the development of new hybrids with desired functionality.[6−9] In this regard, the pillaring of semiconducting sol particles into layered inorganic solids is a promising method for improving catalytic activity because recombination between electrons and holes is effectively suppressed because of electron transfer between guest and host.[10,11] Actually, it was reported that the pillaring of semiconducting materials such as CdS−ZnS, Fe_2O_3, and TiO_2 gives rise to a remarkable enhancement in their photocatalytic activity compared to unsupported catalysts.[11−13] Such photocatalytic activity of semiconductor pillars has also been known to be dependent on the type of the host layer. For example, the CdS−ZnS pillar stabilized in the interlayer space of a layered semiconductor shows much higher photoactivity than that pillared in the insulating host lattice.[11,13]

* To whom correspondence should be addressed. Fax: +82-2-872-9864. Phone: +82-2-880-6658. E-mail: jhchoy@plaza.snu.ac.kr.
† National Nanohybrid Materials Laboratory, Seoul National University.
‡ School of Chemistry and Molecular Engineering, Seoul National University.

(1) Fujishima, A.; Honda, K. *Nature* **1972,** *37,* 238.
(2) Hagfeldt, A.; Grätzel, M. *Chem. Rev.* **1995,** *95,* 49.
(3) Hoffmann, M. R.; Martin, S. T.; Choi, W.; Bahnemann, D. W. *Chem. Rev.* **1995,** *95,* 69.
(4) Ozin, G. *Adv. Mater.* **1992,** *4,* 619.
(5) Lvov, Y.; Ariga, K.; Ichinose, L.; Kunitake, T. *J. Am. Chem. Soc.* **1995,** *117,* 6117.

(6) Choy, J. H.; Kwon, S. J.; Park, K. S. *Science* **1998,** *280,* 1589.
(7) Choy, J. H.; Park, N. G.; Hwang, S. J.; Kim, D. H.; Hur, N. H. *J. Am. Chem. Soc.* **1994,** *116,* 11564.
(8) Choy, J. H.; Kwak, S. Y.; Park, J. S.; Jeong, Y. J.; Portier, J. *J. Am. Chem. Soc.* **1999,** *121,* 1399.
(9) Choy, J. H.; Kwak, S. Y.; Jeong, Y. J.; Park, J. S. *Angew. Chem., Int. Ed.* **2000,** *39,* 4042.
(10) Yanagisawa, M.; Uchida, S.; Fujishiro, Y.; Sato, T. *J. Mater. Chem.* **1998,** *8,* 2835.
(11) Yanagisawa, M.; Sato, T. *Int. J. Inorg. Chem.* **1999,** *1,* 67.
(12) Sato, T.; Yamamoto, Y.; Fujishiro, Y.; Uchida, S. *J. Chem. Soc., Faraday Trans.* **1996,** *92,* 5089.
(13) Uchida, S.; Yamamoto, Y.; Fujishiro, Y.; Watanabe, A.; Ito, O.; Sato, T. *J. Chem. Soc., Faraday Trans.* **1997,** *93,* 3229.

Table 1. Lattice Parameters, Symmetries, and Chemical Formulas of the Layered Host Materials

sample	a (Å)	b (Å)	c (Å)	symmetry	chemical formula
layered cesium titanate	3.823	17.215	2.955	orthorhombic	$Cs_{0.67}Ti_{1.83}\square_{1.83}O_4$
layered protonic titanate	3.752	18.175	2.955	orthorhombic	$H_{0.67}Ti_{1.83}\square_{1.83}O_4 \cdot H_2O$

Despite this advantage of the semiconductor−semiconductor pillar system, it is not easy to construct a semiconducting pillar like TiO_2 in layered titanate or titanoniobate because these types of host materials show no swelling ability. To overcome this shortcoming of layered semiconducting materials, a templating technique was once suggested,[14,15] in which the interlayer spacing of a layered transition metal oxide was preexpanded with long alkylamine chains and then metal oxide sol particles were subsequently introduced. However, the TiO_2-pillared layered titanate prepared by the templating method also exhibits various limitations, such as poor thermal stability, low surface area, and poor crystallinity.[16] These are explicable as a result of the high layer charge of the host lattice which hinders from an effective intercalation of TiO_2 sol particles because the interlayer space of the host layer does not undergo sufficient swelling to permit large guest species to be intercalated. In light of this, we have developed a novel route to generate a well-ordered TiO_2-pillared layered titanate with enhanced photocatalytic activity, which could only be realized by combining two notable steps, namely, the exfoliation of the host titanate layer and its restacking in the presence of well-developed anatase TiO_2 nanosol. Such a hybridization between exfoliated titanate and anatase TiO_2 nanosol at the molecular level is found to be advantageous for the preparation of porous structured material, because it provides a way of accessing guest species freely into the interlayer space of the host lattice without any steric hindrance.[17−20] The driving force for the hybridization reaction might be a kind of van der Waals interaction between tetrabutylamine molecules on the surface of the exfoliated titanate sheet and acetylacetone molecules on TiO_2 nanosol. In this regard, the most important step for hybridization is thought to be that involving the preparation of the monodispersed and nonaggregated TiO_2 nanosol particles. This can be accomplished by using a strong complexing ligand such as acetylacetone because it also plays a role as a blocking agent preventing particle growth.[21]

Experimental Section

Sample Preparation. The host cesium titanate, $Cs_{0.67}Ti_{1.83}\square_{0.17}O_4$, was prepared by heating a stoichiometric mixture of Cs_2CO_3 and TiO_2 at 800 °C for 20 h.[22] The corresponding protonic form, $H_{0.67}Ti_{1.83}\square_{0.17}O_4 \cdot H_2O$,

Table 2. Elemental Analysis (CHNS) of the Host Materials, the Exfoliated Titanate, and the TiO_2-Intercalated Layered Titanate

samples	C (%)	H (%)	N (%)	S (%)
layered cesium titanate	0	0.30	0	0
layered protonic-titanate	0	1.91	0	0
TBA-intercalated titanate[a]	24.56	5.31	1.46	0
TiO_2-intercalated titanate	11.52	2.64	0	0

[a] Tetrabutylamine-intercalated layered titanate, which was obtained by centrifugation (15 000 rpm) of exfoliated titanate solution.

was obtained by reacting the cesium titanate powder with 1 M HCl aqueous solution at room temperature for 3 days. During the proton exchange reaction, the HCl solution was replaced with a fresh one everyday.[23] The layered protonic titanate was exfoliated into single titanate sheets by intercalating TBA (tetrabutylamine) molecules, as reported previously.[24] On the other hand, a monodispersed and nonaggregated TiO_2 nanosol was prepared by adding dropwise titanium isopropoxide (30 mL) with acetylacetone (20.38 mL) to a 0.015 M HNO_3 aqueous solution (180 mL) under vigorous stirring and then peptizing at 60 °C for 8 h.[21] A TiO_2-pillared layered titanate was prepared by hybridizing the exfoliated layered titanate solution with the TiO_2 nanosol at 60 °C for 24 h. The resulting powder was collected by centrifuging (12 000 rpm, 10 min), washed with a mixed solution of distilled water and ethanol (1:1, v/v) to remove excess TiO_2 sol, and dried in ambient atmosphere. Finally, the obtained material was heated at 300 °C for 2 h in order to complete the pillaring process.

Sample Characterization. The crystal structures of the pristine titanate and its derivatives were studied by powder X-ray diffraction (XRD) measurements using Ni-filtered Cu Kα radiation ($\lambda = 1.540\,56$ Å) with a graphite diffracted beam monochromator, and their chemical compositions were determined by performing elemental analysis (ICP & CHNS). As listed in Table 1, the present ICP results indicate that 0.67 mol of cesium ions is incorporated into the crystal lattice, and cesium ions are successfully exchanged with protons by acid treatment. The CHNS analysis data of the pillaring process are summarized in Table 2. No trace of nitrogen was detected for the sample of TiO_2-intercalated layered titanate prepared by hybridizing exfoliated titanate with TiO_2 nanosol, indicating that the tetrabutylamine in the interlayer of titanate was fully exchanged by TiO_2 nanosol coordinated acetylacetone. Therefore, TiO_2-intercalated layered titanate only contains water and acetylacetone as organic species in the interlayer space. Consequently, when the sample is heated at 300 °C for 2 h in air, acetylacetone molecules in the interlayer space could be removed because the boiling point of acetylacetone is known to be ∼140.4 °C. Thermogravi-

(14) Han, Y. S.; Choy, J. H. *J. Mater. Chem.* **1998**, *8*, 1459.

(15) Choy, J. H.; Park, J. H.; Yoon, J. B. *J. Phys. Chem. B.* **1998**, *102*, 5991.

(16) Yanagisawa, M.; Uchida, S.; Yin, S.; Sato, T. *Chem. Mater.* **2001**, *13*, 174.

(17) Bissessur, R.; Heising, J.; Hirpo, W.; Kanatzidis, M. *Chem. Mater.* **1996**, *8*, 318.

(18) Heising, J.; Bonhomme, F.; Kanatzidis, M. G. *J. Solid State Chem.* **1998**, *139*, 22.

(19) Modestov, A.; Glezer, V.; Marjasin, I.; Lev, O. *J. Phys. Chem. B.* **1997**, *101*, 4623.

(20) Wang, L.; Rocci, M.; Brazis, P.; Kannewurf, C. R.; Kim, Y. I.; Lee, W.; Choy, J. H.; Kanatzidis, M. G. *J. Am. Chem. Soc.* **2000**, *122*, 6629.

(21) Scolan, E.; Sanchez, C. *Chem. Mater.* **1998**, *10*, 3217.

(22) Grey, I. E.; Madsen, I. C.; Watts, J. A.; Bursill, L. A.; Kwiatkowska, J. *J. Solid State Chem.* **1985**, *58*, 350.

(23) Sasaki, T.; Komatsu, Y.; Fujiki, Y. *J. Chem. Soc., Chem. Commun.* **1991**, *817*, 2222.

(24) Sasaki, T.; Watanabe, M.; Hashizume, H.; Yamada, H.; Nakazawa, H. *J. Am. Chem. Soc.* **1996**, *118*, 8329.

2488 *Chem. Mater., Vol. 14, No. 6, 2002*

Choy et al.

metric analysis (TGA) was also carried out to check the thermal stability of TiO_2-intercalated titanate with an ambient atmosphere where the heating rate was fixed at 5 °C/min. To determine the surface area and porosity of the samples, the nitrogen adsorption−desorption isotherms were measured volumetrically at liquid-nitrogen temperature with a homemade computer-controlled measurement system.[25] UV−vis spectra measurements were performed to evaluate the photochemical properties of the samples. Diffuse reflectance UV−vis spectra were recorded on a Perkin-Elmer Lamda 12 spectrometer equipped with an integrating sphere of 60 mm in diameter using $BaSO_4$ as a standard. The UV−vis spectra obtained in diffuse reflectance mode [R_∞] were transformed to a magnitude proportional to the extinction coefficient (κ) through the Kubelka−Munk function [$F(R_\infty)$].[26]

$$F(R_\infty) = (1 - R)^2/2R_\infty$$

The band gap energies were determined from the onset of the diffuse reflectance spectra.

Photocatalytic Reaction. Photocatalytic reactions have been carried out in a Pyrex reactor with a capacity of 36 cm^3, which was attached to an inner radiation type 600 W Xe lamp. The inner cell contains thermostated water flowing through a jacket between the Xe lamp and the reaction chamber and is constructed with quartz glass. The catalyst (10 mg) was dispersed in 30 cm^3 of 0.1 M triethanolamine solution by magnetic stirring and was irradiated by a Xe lamp for 20 h. Pt was loaded by a photodeposition method with addition of H_2PtCl_6 into aqueous solution.[12] The photocatalytic activity of the catalyst was determined by measuring the total gas volume of hydrogen evolved during the irradiation of the catalyst suspension in water with a gas buret after confirming the production of hydrogen by gas chromatography HP5890 using a molecular sieve 13X column.

Results and Discussion

Powder XRD Analysis. The powder XRD pattern of the pristine $Cs_{0.67}Ti_{1.83}\square_{0.17}O_4$ is shown in Figure 1, together with that of the proton-exchanged form $H_{0.67}Ti_{1.83}\square_{0.17}O_4 \cdot H_2O$ and the lattice parameters obtained from the least-squares fitting analyses are summarized in Table 1. The XRD feature for the pristine layered cesium titanate is found to be the same as that for the lepidocrocite structure with orthorhombic symmetry. Upon acid treatment, the (020) reflection of the layered cesium titanate is shifted toward a lower angle, indicating lattice expansion due to intercalation of water molecules into the interlayer space of the protonic titanate.

Figure 2 represents the XRD patterns of the selected samples under the pillaring process. From the (020) reflection at $2\theta = 9.6°$ (Figure 2a), the basal spacing of 0.92 nm for the layered protonic titanate could be determined. Before the ion-exchange reaction with TiO_2 nanosol, the layered protonic titanate was exfoliated by intercalating tetrabutylamine. The exfoliated titanate
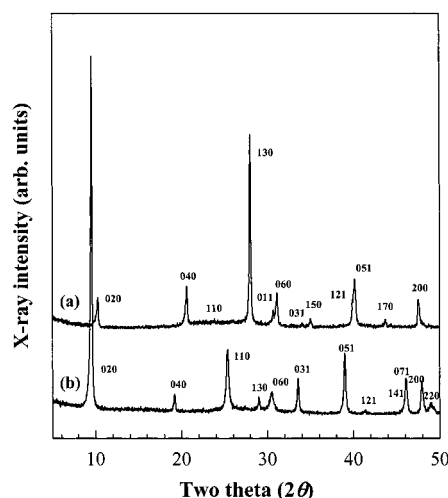
(25) Park, J. H., M.S. Thesis, Seoul National University, Seoul, Korea, 1998.
(26) Anpo, M.; Shima, T.; Kodama, S.; Kubokawa, *J. Phys. Chem.* **1987**, *91*, 4305.

Figure 1. Powder XRD patterns of the layered cesium titanate (a) and the acid-treated sample (b).
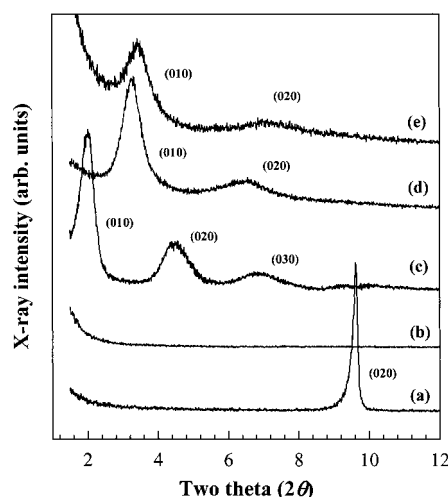

Figure 2. Powder XRD patterns of the layered protonic titanate (a), the colloidal suspension of exfoliated titanate (b), after intercalation of anatase TiO_2 nanosol (c), the TiO_2-pillared layered titanate with heat-treatment at 300 °C (d) and 350 °C (e) for 2 h.

does not show any basal reflections (Figure 2b), indicating that the titanate single sheets are dispersed in aqueous medium.[27] Upon reaction of the exfoliated titanate with anatase TiO_2 nanosol, the (020) reflection of the protonic form is displaced to the (010) reflection of the restacked titanate at a lower angle ($2\theta = 2.1°$ and $d = 4.36$ nm), suggesting that the monodispersed TiO_2 nanosol is stabilized in the interlayer space of layered titanate. The well-developed (0*l*0) peaks at $2\theta = 2.1°$, 4.2°, and 6.3° indicate that the resulting TiO_2-pillared titanate is fairly well ordered along the *b* axis (Figure 2c). After calcinating at 300 °C for 2 h, its basal spacing decreases to 2.56 nm (Figure 2d), which is mainly attributed to the dehydroxylation of pillared TiO_2 nanosol particle and to the pyrolysis of acetylacetone molecules coordinated on the surface of TiO_2 nanosol. Such a pillared structure is maintained even after calcinating at 350 °C for 2 h (Figure 2e), whereas it collapses to an amorphous phase above 400 °C. It is worthwhile to mention here that the thermal stability of layered

(27) Sasaki, T.; Watanabe, M. *J. Am. Chem. Soc.* **1998**, *120*, 4682.

Figure 3. TG and DTG curves for (a) the layered protonic titanate and (b) the TiO$_2$-intercalated layered titanate.
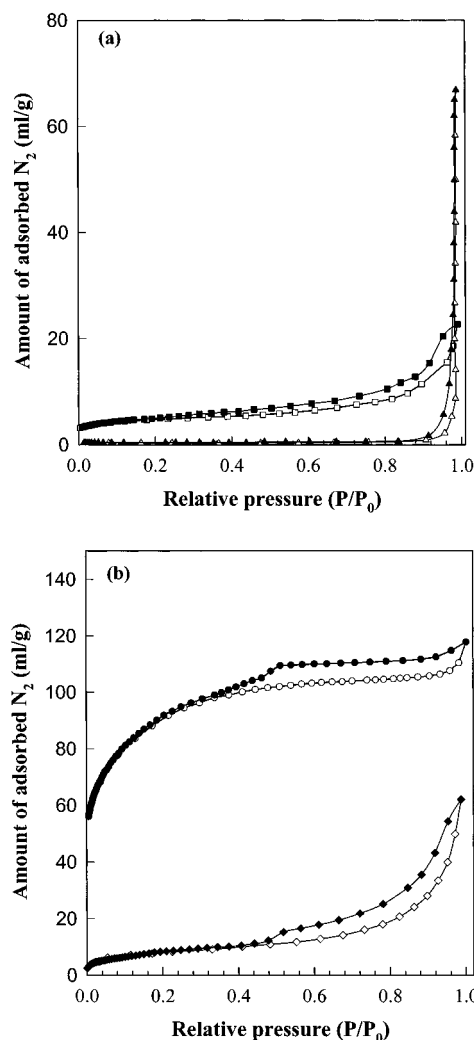

Figure 4. Nitrogen adsorption−desorption isotherms of the pillaring process: the layered cesium titanate (squares), the layered protonic titanate (triangles), the TBA-intercalated layered titanate (diamonds), and the TiO$_2$-pillared layered titanate (circles). The filled and open symbols represent adsorption and desorption data, respectively.

titanate is significantly enhanced by the pillaring of the TiO$_2$ sol particle because of the formation of a covalent bond between the TiO$_2$ particle and layered titanate lattice.

Thermal Analysis. TG-DTG curves of layered protonic titanate and TiO$_2$-intercalated layered titanate are shown in Figure 3. Only one major step corresponding to weight loss is observed in the TG-DTG curves of layered protonic titanate, which originates from the dehydration of water in the interlayer space of layered titanate (Figure 3a). It was reported that the titanate layers collapsed to produce anatase and rutile phases after complete dehydration, indicating that the layered protonic titanate is thermally unstable.[28] Figure 3b represents the TG-DTG curves of TiO$_2$-intercalated layered titanate, and its weight loss is found to be extend over a wide temperature range because of the combination of several factors contributing to weight decrease such as dehydration, decomposition, and dehydroxylation. The first step up to ∼120 °C is certainly due to the dehydration of water in the titanate layers, and the second step between 120 and 260 °C is attributed to the oxidative decomposition of acetylacetone on the TiO$_2$ surface in the interlayer space of titanate.

The third step beyond 280 °C is due to the dehydroxylation of the TiO$_2$ sol in the host layer. All of the results obtained allow us to confirm that the tetrabutylamine in the titanate layer is completely replaced with the TiO$_2$ nanosol coordinated with acetylacetone and that the thermal stability of the host layer is remarkably enhanced by pillaring of TiO$_2$ sol particles. However, we found that the pillared structure could be collapsed beyond 400 °C and be slowly transformed into the anatase phase without any weight loss.

Nitrogen Adsorption−Desorption Isotherms. Figure 4a represents the nitrogen adsorption−desorption isotherm for the pristine layered cesium titanate and its protonated derivative. The adsorption isotherms for both compounds can be assigned as type III, which is characteristic of nonporous or macroporous solids in the BDDT classification.[29] The desorption curve in Figure 4a also shows a slight hysteresis, probably because of the formation of a house-of-cards structure between neighboring titanate layers. The nitrogen adsorption−

(28) Yin, S.; Uchida, S.; Fujishiro, Y.; Aki, M.; Sato, T. *J. Mater. Chem.* **1999**, *9*, 1191.

(29) Gregg, S. J.; Sing, K. S. W. *Adsorption, Surface Area and Porosity*; Academic Press: London, 1982.

Table 3. Specific Surface Areas, Pore Volumes, and Pore Diameters of the Layered Titanate and the TiO$_2$-Pillared Layered Titanate

sample identification	surface area (m^2/g)		pore volume (mL/g)		pore diameter (Å)^b
	S_{BET}	$S_{Langmuir}$	$V_{total}{}^a$	$V_{micro}{}^b$	
layered cesium titanate	1	1	0	0	0
layered protonic titanate	13	24	0	0	0
TBA-intercalated layered titanate	24	51	0	0	0
TiO$_2$-pillared layered titanate 200 °C	233	380	0.147	0.096	3.7
TiO$_2$-pillared layered titanate 300 °C	251^c	458^c	0.171	0.153	9.5
TiO$_2$-pillared layered titanate 400 °C	72	147	0.075	0.063	17.2

^{a} Specific total pore volume at $P/P_0 = 0.98$. ^{b} Estimated by t plot method. ^{c} The correlation coefficient ($R = 0.9981$) of $S_{Langmuir}$ is more similar to 1 than that ($R = 0.9936$) of S_{BET}.

desorption isotherm for TiO$_2$-pillared layered titanate calcined at 300 °C for 2 h is shown in Figure 4b in comparison with that of the TBA-intercalated layered titanate. The TBA-intercalated layered titanate exhibits a slightly larger surface area than the pristines of Figure 4a because of the intercalation of organic species for the exfoliation of titanate layers. The TiO$_2$-pillared layered titanate prepared by the reaction of anatase TiO$_2$ nanosol with exfoliated titanate could be type I and/or IV in the BDDT classification (Figure 4b), which is characteristic of microporous adsorbents. In addition, the hysteresis loop resembles H4 in the IUPAC classification,[29] where the loop indicates the presence of open slit-shaped pores with fairly wide bodies and narrow short necks. Such a finding allows us to conclude that the TiO$_2$-pillared layered titanate is analogous to a micropore structure.

As shown in Table 3, the surface area and total pore volume of the TiO$_2$-pillared layered titanate are greatly increased upon pillaring the anatase sol in the layered cesium titanate. The adsorption isotherms give a better fit to the Langmuir equation than the BET one, indicating that the monolayer nitrogen adsorption takes place because of the restricted pore dimensions. The layered cesium titanate has a very low Langmuir surface area of ∼1 m^2/g which is due to its nonporous character. The large Langmuir surface area of TiO$_2$-pillared layered titanate is determined to be ∼460 m^2/g, which is the largest surface area among the same kind of pillared transition metal oxides so far reported. Such a large enhancement is attributed to the presence of fairly well-ordered TiO$_2$ sols in the interlayer space of layered titanate created by the pillaring process. The micropore volume (V_{micro}) and approximate pore diameter ($2t$) can be calculated from the t plot.[30] The line extrapolated from the high-pressure branch to the adsorption axis gives an intercept, which is equivalent to the micropore volume. The pore diameter can also be estimated from the inflection point of the t plot by multiplying the t value corresponding to this inflection point by a factor of 2. The pore volumes and pore diameters for the pillaring process of layered titanate are summarized in Table 3. From these values, it is evident that ca. 90% of the total pore volume in TiO$_2$-pillared layered titanate is composed of micropores.

The pore size distribution curve of the TiO$_2$-pillared layered titanate calcined at 300 °C for 2 h is calculated by the micropore analysis (MP) method (Figure 5), which is based on the t plot.[31] It becomes clear that the
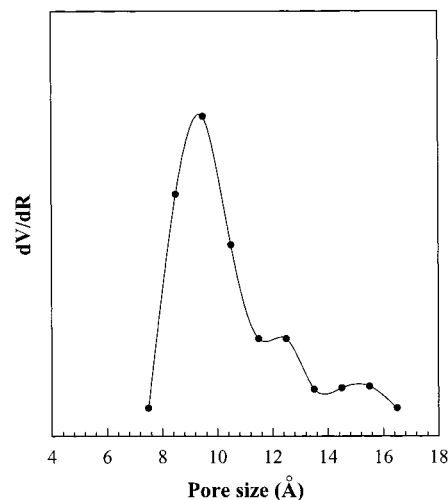

Figure 5. Pore size distribution curve for the TiO$_2$-pillared titanate calcined at 300 °C for 2 h.

TiO$_2$-pillared layered titanate mainly consists of micropores with a size of ∼0.95 nm. From the present XRD data (Figure 2d), it can be assumed from the basal spacing that the pillared material has a mesoporosity with a large gallery height of 2.56 nm. However, the adsorption data strongly support the formation of micropores in the TiO$_2$-pillared layered titanate. Such results can be understood based on the stacking model of multilayered nanosol particles where micropores are formed among sol particles as previously reported.[15,32,33]

UV−vis Spectroscopy. Figure 6 shows the UV−vis diffuse reflectance spectrum of the TiO$_2$-pillared layered titanate, which is compared with those of the layered protonic titanate and anatase TiO$_2$. One important feature of the reflectance spectra is a red shift in the onset of the spectra as a result of hybridizing the layered protonic titanate with anatase TiO$_2$ nanosol. The layered protonic titanate has a band gap energy of ∼3.5 eV, which is determined by the onset of reflectance spectra. By reacting the anatase TiO$_2$ nanosol, the layered protonic titanate band was shifted to a longer wavelength region corresponding to a band gap energy of ∼2.7 eV. This is attributed to the formation of bonds between the host layer and anatase TiO$_2$. Similar results were also reported for iron oxide-pillared montmorillonite,[34,35] titanium oxide-pillared montmorillonite,[36] silicon oxide/titanium oxide-pillared montmorillonite,[15] and various cadmium sulfide/zinc sulfide-pillared layered compounds.[11,37,38]

(30) Allen, T. *Particle Size Measurement*, 4th ed.; Chapman and Hall: London, 1980.

(31) Mikhail, R. S.; Brunauer, S.; Bodor, E. E. *J. Colloid Interface Sci.* **1968**, *26*, 45.

(32) Han, Y. S.; Yamanaka, S.; Choy, J. H. *J. Solid State Chem.* **1999**, *144*, 45.

(33) Han, Y. S.; Matsumoto, H.; Yamanaka, S. *Chem. Mater.* **1997**, *9*, 2103.
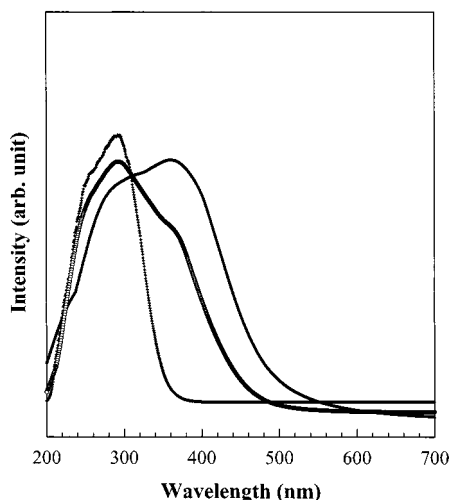
Figure 6. Diffuse UV−vis spectra for the layered protonic titanate (+), the TiO$_2$-pillared layered titanate (●), and the anatase TiO$_2$ nanosol (▲).

Figure 7. Cumulative amount of hydrogen gas evolved from a 30 cm^3 solution of 1.0 M triethanolamine containing 10 mg of the dispersed layered cesium titanate (square), the layered protonic titanate (diamond), the anatase TiO$_2$ particle (triangle), the TiO$_2$-pillared layered titanate (circle), and the Pt (0.3 wt %)-doped TiO$_2$-pillared layered titanate (filled circle). The inset shows the time development of H$_2$ gas evolved without Pt loading.

Photocatalytic Activity. The photocatalytic activity of the pillared material was evaluated by measuring the total volume of hydrogen gas evolved during the irradiation of the catalyst suspensions in water. We found that the amount of H$_2$ gas evolved increases according to the following order: layered titanate (cesium and protonic form) < unsupported TiO$_2$ (acac-TiO$_2$) < TiO$_2$-pillared layered titanate (inset of Figure 7). Compared to the pristine layered cesium titanate (2.00 μM h^{-1}), the TiO$_2$-pillared titanate shows higher catalytic activity (8.68 μM h^{-1}) because the electron−hole recombination is effectively suppressed because of electron transfer between guest and host. Further enhancement of photocatalytic activity was achieved when Pt was loaded on the TiO$_2$-pillared layered titanate. Pt was deposited on the surface of TiO$_2$-pillared layered titanate by stirring the pillared sample (0.2 g) in 0.24 mM H$_2$PtCl$_6$ aqueous solution (500 mL) at room temperature for 3 days. After being filtered and washed with water, the specimen was dispersed in water and irradiated with UV light from a 600 W Xe lamp at room temperature for 3 h. Surprisingly, a marked enhancement in activity by ca. 40 times was obtained for the TiO$_2$-pillared layered titanate, compared to the pristine compounds such as layered cesium titanate and anatase TiO$_2$ nanosol, when Pt (0.3 wt %) was doped on the surface of the pillared sample (Figure 7). Such an outstanding catalytic effect might be due to the fact that photoexcited holes take part in the oxidation of intercalated water molecules in the TiO$_2$-pillared layered titanate and the
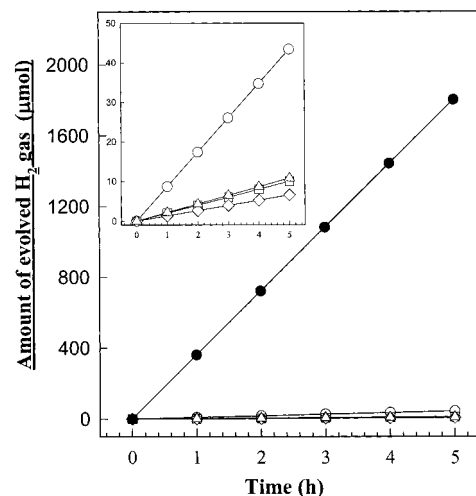
photoinduced electrons could effectively reduce the H$^+$ on the surface of Pt to enhance the formation of H$_2$.[39]

Conclusion

A new microporous TiO$_2$-pillared layered titanate was successfully prepared through an exfoliation-restacking route. The TiO$_2$-pillared layered titanate exhibited the highest surface area (460 m^2/g) and the most exceptional thermal stability, up to 350 °C, ever reported among semiconductor-pillared transition metal oxides. According to the nitrogen adsorption isotherm measurement, we found that the present pillared material consisted mainly of micropores. On the basis of the above results, a model for multilayer-stacked interlayer sol particles is proposed in which the pillars between sol particles and titanate layers provide a unique micropore structure. A remarkable enhancement in activity by ca. 40 times was obtained for the Pt-doped TiO$_2$-pillared layered titanate compared to the pristine compound.

Supporting Information Available: Figures detailing our results (PDF). This material is available free of charge via the Internet at http://pubs.acs.org.

CM010815M

(34) Miyoshi, H.; Yoneyama, H. *J. Chem. Soc., Faraday Trans. 1* **1989**, *85*, 1873.
(35) Miyoshi, H.; Mori, H.; Yoneyama, H. *Langmuir* **1991**, *7*, 503.
(36) Yoneyama, H.; Haga, S.; Yamanaka, S. *J. Phys. Chem.* **1989**, *93*, 4833.
(37) Enea, O.; Bard, A. J. *J. Phys. Chem.* **1986**, *90*, 301.
(38) Sato, T.; Okuyama, H.; Endo, T.; Shimada, M. *React. Solids* **1990**, *8*, 63.

(39) Yoshimura, J.; Ebina, Y.; Kondo, J.; Domen, K. *J. Phys. Chem.* **1993**, *97*, 1970.